pISSN 1229-3008 eISSN 2287-6251
Progress in Superconductivity and Cryogenics
Vol.22, No.1, (2020), pp.12~16 https://doi.org/10.9714/psac.2020.22.1.012

A simulation-based design study of superconducting zonal shim coil for a 9.4 T whole-body MRI magnet

Geonyoung Kim, Kibum Choi, Jeonghwan Park, Uijong Bong, Jeseok Bang*, and Seungyong Hahn

Department of Electrical and Computer Engineering, Seoul National University, Seoul, 08826, Korea

(Received 6 March 2020; revised or reviewed 29 March 2020; accepted 30 March 2020)

Abstract

As high homogeneity in magnetic field is required to increase the resolution of MRI magnets, various shimming methods have been researched. Using one of them, the design of the superconducting active zonal shim coil for MRI magnets is discussed in this paper. The magnetic field of the MRI magnet is expressed as the sum of spherical harmonic terms, and the optimized current density of shim coils capable of removing higher-order terms is calculated by the Tikhonov regularization method. To investigate all potential designs derived from calculated current density, 4 sweeping parameters are selected: (1) axial length of shim coil zone; (2) radius of shim coils; (3) exact axial position of shim coils; and (4) operating current. After adequate designs are determined with constraints of critical current margin and homogeneity criterion, the total wire length required for each is calculated and the design with a minimum of them is chosen. Using the superconducting wire length of 9.77 km, the field homogeneity over 50 cm DSV is improved from 24 ppm to 1.87 ppm in the case study for 9.4 T whole-body MRI shimming. Finally, the results are compared with the finite element method (FEM) simulation results to validate the feasibility and accuracy of the design.

Keywords: active shim coil, magnetic field homogeneity, parameter sweep

1. INTRODUCTION

Magnetic resonance imaging (MRI) technology has been developed for medical diagnosis and scientific research. High field MRI systems that reach the magnetic flux density of 7 T, 9.4 T or even 11.7 T are having been established since they allow to increase the resolution with detecting not only hydrogen but also carbon, phosphorous, or oxygen [1-3].

As uniform field homogeneity in the magnetic field is crucial to improve the resolution of MRI magnets, many different types of shimming methods have been researched [4-13]. Superconducting active shim coil to mitigate the magnetic field inhomogeneity [14-17] is one of the potential options, mainly because it may operate higher current density which makes it possible to manipulate the worse inhomogeneity than the normal wire [18-21].

Shim coils are also classified as zonal shim coil and tesseral shim coil depending on the components of spherical harmonic terms, and usually, both are required. As the screening current occurring in REBCO tape mainly increases the error in zonal components [22], we aimed to design zonal shim coil in this paper. In a conventional shim coil design process, each coil set, operating with individual power supplies, mitigates each harmonic coefficient terms. This method may have a disadvantage since the practical shim coils not only remove the target harmonic components but also create the error in other component. For this reason, a shimming method which enables canceling of multiple harmonic coefficient terms only with one series of coil sets is being researched recently [23-24].

Here, we propose a design method for active zonal shim coil which can simultaneously remove both low and high order harmonics using Tikhonov regularization together with parameter sweep approach. We calculate the surface current density which cancels the harmonic components and find a practical design that can do the same. To figure out the optimized design of active shim coil, four sweeping parameters are selected: 1) axial length of shim coil zone; 2) radius of shim coils; 3) exact axial positions of shim coils; and 4) operating current. Considering construction limits, turns of each shim coils, axial positions, and operating current are quantized. Each design's critical current margin and field homogeneity is computed with analytic calculation and the design with the minimum amount of wire consumption is chosen. Finally, the design properties from the analytic calculation are compared with the finite element method simulation results, and then the feasibility and the accuracy of the design was evaluated.

2. DESIGN METHODOLOGY

2.1. Method for Calculating Surface Current Density of an Ideal Active Shim coil: Tikhonov regularization

Zonal shim coil is designed to lay on the surface of the cylinder which has an axial length of *2L* and a radius of a as shown in Fig. 1.(a). We set the target region along the z-axis from pL to qL ($-a/L \leq p < q \leq a/L$). Spherical harmonic coefficients for this region are calculated and surface current density erasing these terms is obtained.

* Corresponding author: jeseoknim@snu.ac.kr

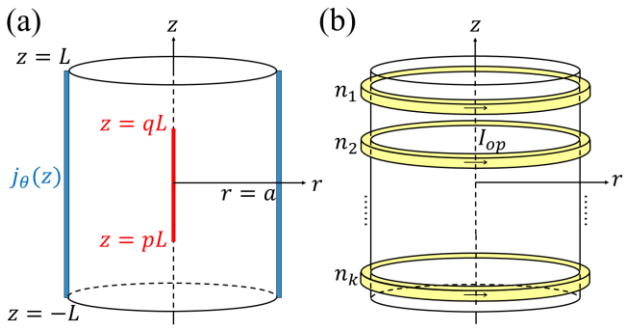

Fig. 1. (a) A schematic diagram of geometric parameters for calculating surface current density. Thick red line stands for the target region and blue area represents surface current density, $j_\theta(z)$. (b) A schematic diagram for a particular shim coil with construction limits considered. $n_1, \cdots, n_k$ refers to each coil's turns and I_{op} refers to the operating current.

In the first cut design stage, we assume the shim coil is continuously located along the surface of the cylinder and the thickness of the coil is negligible. Also current is supposed to flow only in the azimuthal direction. Then the current density can be treated as a surface current density $j_\theta(z)$, and then the axial magnetic field along the axis is calculated by Biot-Savart law. As the tesseral shimming is not considered in this paper, the field along the axis is sufficient. To compute optimized surface current densities mitigating spherical harmonic coefficients induced by an MRI magnet, Tikhonov regularization method which is one of the error minimization methods using Lagrange Multiplier is adopted [23].

Suppose that the surface current density consists of the sums of basis functions defined by sine functions.

$$j_\theta'(z) = \sum_1^N P_m \sin\left(\frac{m\pi(z+L)}{2L}\right), -L < z < L. \quad (1)$$

N stands for the number of basis terms and P_m is coefficients for basis function. $j_\theta{}'(z)$ becomes $j_\theta(z)$ as $N \to \infty$. Substituting (1) into Maxwell's equations gives the conclusion as the following.

$$H_z'(z) = -\sum_1^N P_m T_m(z)\ , \quad pL < z < qL. \quad (2)$$

$$T_m(z) = -\int_{-L}^{L} \frac{a^2}{(a^2+(z'-z)^2)^{\frac{3}{2}}} \sin\left(\frac{m\pi(z'+L)}{2L}\right) dz'. \quad (3)$$

$H_z'(z)$, the approximated magnetic field, becomes an actual magnetic field $H_z(z)$ as $N \to \infty$, but, because N is a finite positive integer, $H_z'(z)$ makes some error. To minimize this error, the governing function from the Tikhonov regularization method is defined. Then the partial derivative of governing function with respect to each P_m $(m = 1, \cdots, N)$ should be zero, so this leads to the following expressions.

$$\sum_{m=1}^N S_{n,m} P_m = -\int_{pL}^{qL} H_z(z)\, T_n(z) dz. \quad (4)$$

$$S_{n,m} = \int_{pL}^{qL} T_n(z) T_m(z) dz + \delta_{n,m} \frac{n^4\pi^4\lambda}{16L^3}. \quad (5)$$

$\delta_{n,m}$ stands for the Kronecker delta function. λ is a regularization parameter, and setting it small enough can reduce the error. P_m can be determined by solving (4) and $j_\theta{}'(z)$ is also determined from (1).

2.2. Actual Shim Coil Design Process with Construction Limit Considered: Parameter Sweep Approach

Using (2) and (3), we can express a given magnetic field along the axis with the superposition of the magnetic field of ideal circular current loops. By applying the Gaussian quadrature for magnetic field formula, the axial magnetic field can be expressed as the superposition of ideal loop currents.

$$H_z(z) = \sum_{i=1}^k w_i j_\theta(z_i) \frac{a^2}{(a^2+(z_i-z)^2)^{\frac{3}{2}}}, \quad (6)$$

where z_i and w_i respectively stand for the i^{th} Gaussian quadrature nodes and weights. k is the total amount of current loops. z_i determine the axial positions of shim coils and w_i determine the turns and operating current.

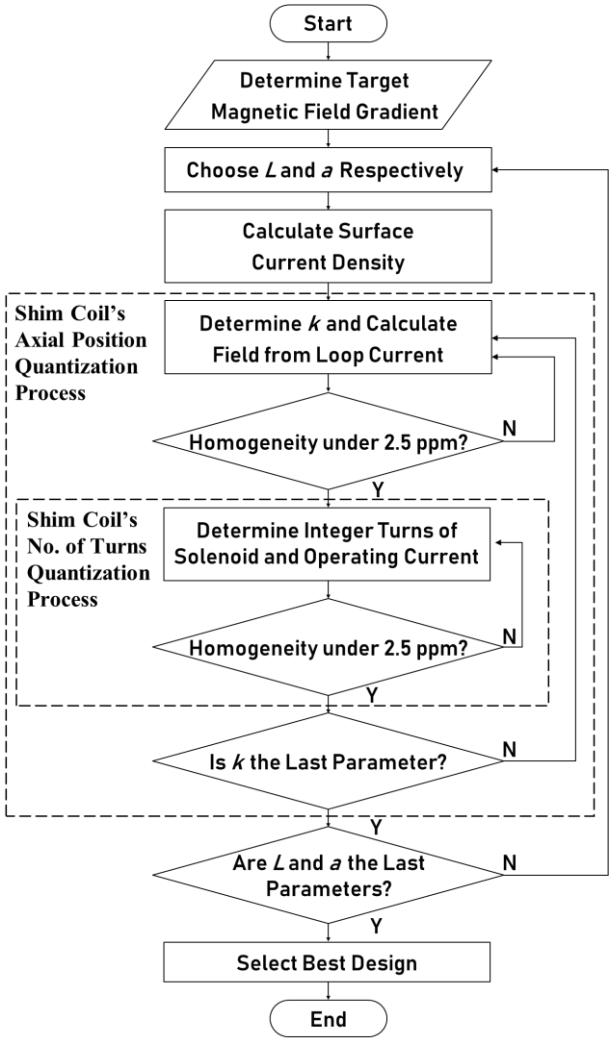

Fig. 2. A flowchart of parameter sweep approach for active zonal shim coil design.

In this design step, we assume that the current is flowing through the solenoid with a square cross-section. Since the ideal loop current which is calculated in the previous step and solenoid generate different magnetic field gradient, the parameter sweep method is chosen to find out the adequate coil design for creating uniform field homogeneity. Each solenoid is supposed to have integer turns $(n_1, \cdots, n_k)$ and the sign of turns means the direction of the current. Every solenoid is driven by one operating current I_{op} as shown in Fig. 1. (b).

Four sweeping parameters are selected: 1) height of shim coil zone determined by L; 2) radius of shim coils, a; 3) exact axial positions of shim coils which are determined by k; and 4) operating current. Among the potential shim coil models, critical current margin and field homogeneity are considered to figure out the satisfactory models [25]. Then, the total wire length required for each one is calculated and the design with a minimum length is chosen. The whole process of parameter sweeping is presented in Fig. 2.

3. CASE STUDY: 9.4 T WHOLE-BODY MRI ZONAL SHIM COIL DESIGN

To verify our shim coil design method, designed MRI magnet by other work [1] is adopted as a reference. Since the proposed 9.4T MRI magnet design has a bore size of 100 cm and an axial length of 200 cm, the range of shim coil axial length ($2L$) and radius (a) are respectively set to < 100 cm and 45~48 cm. Shim coils are designed to be located inside the magnet bore and also they have to be located in the cryostat. The field homogeneity over 50 cm DSV measured in [1] is 24 ppm peak to peak. As the magnet is designed to be symmetric, only even number components of the harmonic coefficients are considered.

Results of parameter sweep process are presented in Fig. 3. Shim coil's cross-section is assumed to be a square with a 10 mm side length. Parameter sweep area for L ranges from 980 mm to 1000 mm and the area for a ranges from 450 mm to 480 mm, calculated at 1 mm intervals each. Field homogeneity criterion is below 2 ppm.

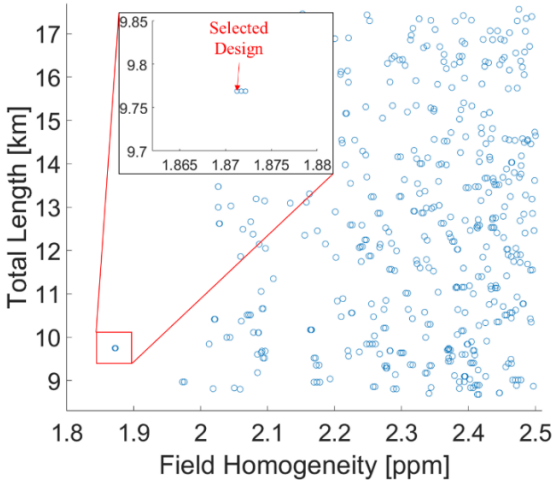

Fig. 3. The scatter plot of the results of parameter sweep. The x-axis represents the field homogeneity over 50 cm DSV and the y-axis represents the total required length of wire. The selected design is marked in the enlarged area, the red box.

TABLE I
KEY PARAMETERS OF ACTIVE ZONAL SHIM COIL DESIGN.

Parameters	Values
Height of shim coil zone ($2L$) [mm]	1990
Shim coil inner radius [mm]	455
Shim coil outer radius [mm]	465
Shim coil thickness [mm]	10
Number of shim coils (k) [-]	29
Operating current [A]	176.89
Total turns [-]	3380
Total wire length [km]	9.77
Field homogeneity over 50cm DSV [ppm]	1.87

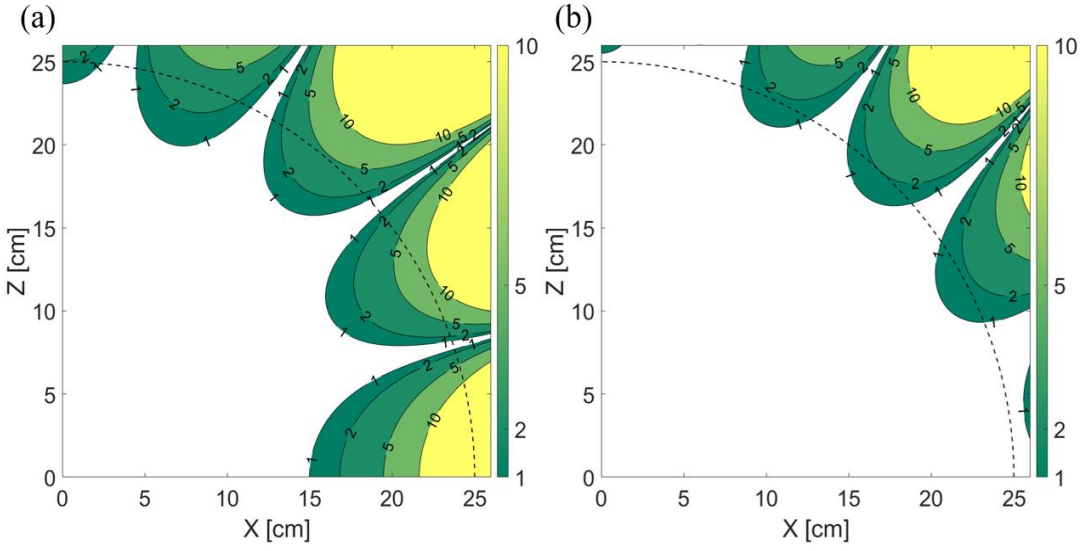

Fig. 4. (a) Magnetic field homogeneity contour plot on the first quadrant of the XZ plane without shim coils, (b) Magnetic field contour plot on XZ plane (Y=0) with shim coils. The dashed line stands for the 50 cm DSV sphere. In each figure, contour levels for the magnetic field are determined to 1, 2, 5, and 10 ppm. The innermost blank region colored with white represents sub-ppm-level.

TABLE II
COEFFICIENTS OF SPHERICAL HARMONIC EXPANSION BEFORE AND AFTER SHIMMING.

Name	Value [ppm]	
	Before shimming	After shimming
Z2	0.68	0.22
Z4	1.1	0.65
Z6	5.7	0.09
Z8	11.7	2.3

Considering the permanent joint of wire, Bi2212 can be chosen as wire material [26]. Since the critical current is measured to be around 300 A [27-28], the operating current below 200A at 9.4T will have a sufficient margin.

The key parameters from the analytic calculation are summarized in Table I. The operating current is calculated to be 176.89 A which makes more than 30 % of margin in critical current density. Total superconducting wire consumption is 9.77 km and the field homogeneity over 50 cm DSV is improved to 1.87 ppm peak to peak.

As mentioned in Table II, spherical harmonic coefficients are decreased after shimming. Coefficients for Z2 and Z4 are reduced respectively to one third and to almost half, and those of Z6 and Z8 are drastically reduced.

Contour plots in Fig. 4. surrounding the 50 cm DSV sphere shows that the field homogeneity is improved after shimming. The magnetic field inside the 50 cm DSV sphere is calculated and the field inhomogeneity is expressed in ppm units. Especially 1 ppm contour line which intrudes the sphere line in Fig. 4.(a) is much uniformly distributed in Fig. 4.(b).

The results with analytic calculation are compared with those from the finite element method (FEM). Calculation of field homogeneity with the FEM method deduced similar results to analytic calculation results. Field homogeneity over 50 cm DSV computed by FEM is 1.88 ppm peak to peak. We can figure out that FEM results validate good agreement with analytic parameter sweep calculation results.

4. DISCUSSION

Improved field homogeneity with canceling the magnetic field harmonic coefficients will lead to the higher resolution of magnetic resonance images. Since the turns of each shim coils, operating current, and coil's axial positions are normalized for satisfying construction limits in this paper, the design parameters such as field homogeneity or total required wire length can be partly irregular or unpredictable. Nonetheless, the magnets with accurate parameters from which the exact spherical harmonic coefficients can be measured are able to be sufficiently shimmed with this method. Additional case studies or experiments for real magnets or asymmetric field gradients will provide further verification of this work.

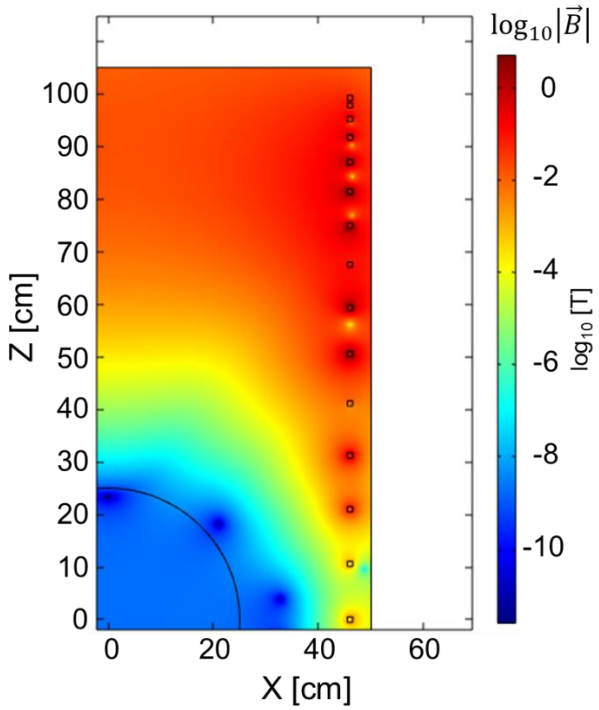

Fig. 5. FEM simulation result on the first quadrant of the XZ plane. Log scale of a magnetic field created by only shim coil inside the MRI magnet's bore is expressed.

5. CONCLUSION

A parameter sweep approach for superconducting active zonal shim coil based on the Tikhonov regularization method is proposed in this paper. The properties of shim coils are defined with four parameters including axial length of shim coils, a radius of coils, the exact axial position of shim coils, and operating current. Nb_3Sn or Bi2212 are considered to construct the shim coils because these materials can operate in a high magnetic field and are also possible for the permanent joint. Using the suggested design method, superconducting active zonal shim coil for a proposed 9.4 T MRI magnet is deduced. Required total wire length is measured to 9.77 km and field homogeneity over 50 cm DSV is improved from 24 ppm to 1.87 ppm. The design result is compared with finite element method simulation and the feasibility and accuracy are verified.

ACKNOWLEDGMENT

This work was supported by Samsung Research Funding & Incubation Center of Samsung Electronics under Project Number SRFC-IT1801-09. It was also supported by the BK21 Plus Project in 2019.

REFERENCES

[1] H. Miyazaki, S. Iwai, Y. Otani, M. Takahashi, T. Tosaka, K. Tasaki, S. Nomura, T. Kurusu, H. Ueda, S. Noguchi, A. Ishiyama, S. Uraama, and H. Fukuyama, "Design of a conduction-cooled 9.4T

REBCO magnet for whole-body MRI systems," *Supercond. Sci. Technol*. 29, 104001, 2016

[2] Y. Dai, Q. Wang, C. Wang, L. Li, H. Wang, Z. Ni, S. Song, S. Chen, B. Zhao, H. Wang, Y. Li, X. Hu, C. Cui, J. Cheng, Y. Lei, and L. Yan, "Structural Design of a 9.4 T Whole-Body MRI Superconducting Magnet," *IEEE Trans. Appl. Supercond*., vol. 22, no. 3, 4900404, June, 2012

[3] J. J. Du, P. Yuan, W. Wu, L. Z. Ma, and X. L. Yang, "Active Shim Design of a 7 T Highly Homogeneous Superconducting Magnet for Lanzhou Penning Trap," *IEEE Trans. Appl. Supercond*., vol. 22, no. 3, 4902004, June, 2012

[4] D. I. Hoult and R. Deslauriers, "Accurate Shim-Coil Design and Magnet-Field Profiling by a Power-Minimization-Matrix Method," *J. Magn. Reson*., Series A 180, pp.9-20, 1994

[5] C. Juchem, B. Muller-Bierl, F. Schick, N. K. Logothetis, and J. Prfeuffer, "Combined passive and active shimming for in vivo MR spectroscopy at high magnetic fields," *J. Magn. Reson*., 183, pp.278-289, 2006

[6] R. Vadovic, "Magnetic Field Correction Using Magnetized Shims," *IEEE Trans. Magn*., vol. 25, no. 4, pp.3133-3139, 1989

[7] L. K. Forbes, M. A. Brideson, and S. Crozier, "A Target-Field Method to Design Circular Biplanar Coils for Asymmetric Shim and Gradient Fields," *IEEE Trans. Magn*., vol. 41, no. 6, pp.2134-2144, 2005

[8] H. S. Lopez, F. Liu, E. Weber, and S. Crozier, "Passive Shim Design and a Shimming Approach for Biplanar Permanent Magnetic Resonance Imaging Magnets," *IEEE Trans. Magn*., vol. 44, no. 3, pp.394-402, 2008

[9] S. Hahn, M. Ahn, J. Bascunan, W. Yao, and Y. Iwasa, "Nonlinear Behavior of a Shim Coil in an LTS/HTS NMR Magnet With an HTS Insert Comprising Double-Pancake HTS-Tape Coils," *IEEE Trans. Appl. Supercond.*, vol. 19, no. 3, pp.2285-2288, June, 2009

[10] G. Hu, Z. Ni, and Q. Wang, "A Novel Target-Field Method Using LASSO Algorithm for Shim and Gradient Coil Design," *IEEE Trans. Appl. Supercond.*, vol. 22, no. 3, 4900604, June, 2012

[11] G. Hu, Z. Ni, and Q. Wang, "Shim Coil Set for NMR Using a Novel Target Field Method Based on Trigonometric Series," *IEEE Trans. Appl. Supercond*., vol. 24, no. 3, 4302105, June, 2014

[12] M. Weiger and T. Speck, "Shimming for high-resolution NMR spectroscopy," *eMagRes*., pp.4468-4486, 2011

[13] P. Hudson, S. D. Hudson, W. B. Handler, and B. A. Chronik, "Finite-Length Shim Coil Design Using a Fourier Series Minimum Inductance and Minimum Power Algorithm," *Concepts Magn. Reson.* Part B. 37, pp.245–253, 2010

[14] M. Ahn, S. Hahn, and H. Lee, "3-D Field Mapping and Active Shimming of a Screening-Current-Induced Field in an HTS Coil Using Harmonic Analysis for High-Resolution NMR Magnets," *IEEE Trans. Appl. Supercond*., vol. 23, no. 3, 4400804, June, 2013

[15] S. Chen, T. Xia, Z. Miao, L. Xu, H. Wang, and S. Dai, "Active shimming method for a 21.3 MHz small-animal MRI magnet," *Meas. Sci. Technol*. 28, 055902, 2017

[16] J. Du, P. Yuan, L. Ma, W. Wu, and X. Yang, "A novel design methodology for active shim coil," *Meas. Sci. Technol*. 23, 085502, 2012

[17] P. Konzbul and K. Sveda, "Shim coils for NMR and MRI solenoid magnets," *Meas. Sci. Technol*. 6, pp.1116-1123, 1995

[18] Z. Ni, L. Li, G. Hu, X. Hu, F. Liu, and Q. Wang, "Design of Superconducting Shim Coils for a 400 MHz NMR Using Nonlinear Optimization Algorithm," *IEEE Trans. Appl. Supercond*., vol. 22, no. 3, 4900505, June, 2012

[19] S. Iguchi, Y. Yanagisawa, M. Takahashi, T. Takao, K. Hashi, S. Ohki, G. Nishijima, S. Matsumoto, T. Noguchi, R. Tanaka, H. Suematsu, K. Saito, and T. Shimizu, "Shimming for the 1020 MHz LTS/Bi-2223 NMR Magnet," *IEEE Trans. Appl. Supercond*., vol. 26, no. 4, 4303507, June, 2016

[20] X. Zhu, Q. Wang, Y. Li, Y. Hu, W. Chen, and F. Liu, "The Design of Decoupled Even-Order Zonal Superconducting Shim Coils for a 9.4 T Whole-Body MRI," *IEEE Trans. Appl. Supercond*., vol. 26, no. 8, 4403708, December, 2016

[21] C. Niu, X. Zhu, Q. Wang, Y. Li, F. Tang, and F. Liu, "A Novel Design Method of Independent Zonal Superconducting Shim Coil," *IEEE Trans. Appl. Supercond*., vol. 29, no. 1, 4400108, December, 2019

[22] S. Iguchi, R. Piao, M. Hamada, S. Matsumoto, H. Suematsu, T. Takao, J. Li, X. Jin, M. Takahashi, H. Maeda, and Y. Yanagisawa, "Advanced field shimming technology to reduce the influence of a screening current in a REBCO coil for a high-resolution NMR magnet," *Supercond. Sci. Technol*. vol. 29, 045013, 2016

[23] L. K. Forbes and S. Crozier, "A novel target-field method for finite-length magnetic resonance shim coils: I. Zonal shims," *J. Phys. D: Appl. Phys.* 34, pp.3447-3455, 2001

[24] L. K. Forbes and S. Crozier, "A novel target-field method for finite-length magnetic resonance shim coils: II. Tesseral shims," *J. Phys. D: Appl. Phys*. 35, pp.839-849, 2002

[25] B. J. Parkinson, R. Slade, M. J. D. Mallett, and V. Chamritski, "Development of a Cryogen Free 1.5 T YBCO HTS Magnet for MRI," *IEEE Trans. Appl. Supercond*., vol. 23, no. 3, 4400405, June, 2013

[26] G. D. Brittles, T. Mousavi, C. R. M. Grovenor, C. Aksoy, and S. C. Speller, "Persistent current joints between technological superconductors," *Supercond. Sci. Technol*. vol. 28, 093001, 2015

[27] H. Miao, K. R. Marken, M. Meinesz, B. Czabaj, and S. Hong, "Development of Round Multifilament Bi-2212/Ag Wires for High Field Magnet Applications," *IEEE Trans. Appl. Supercond*., vol. 15, no. 2, pp.2554-2557, June, 2005

[28] H. Miao, K. R. Marken, M. Meinesz, B. Czabaj, S. Hong, A. Twin, P. Noonan, U. P. Trociewitz, and J. Schwartz, "High Field Insert Coils from Bi-2212/Ag Round Wires," *IEEE Trans. Appl. Supercond*., vol. 17, no. 2, June, 2007